# Testing of radiation boundary conditions in BDY module in NEMO

October 2013

D. Storkey

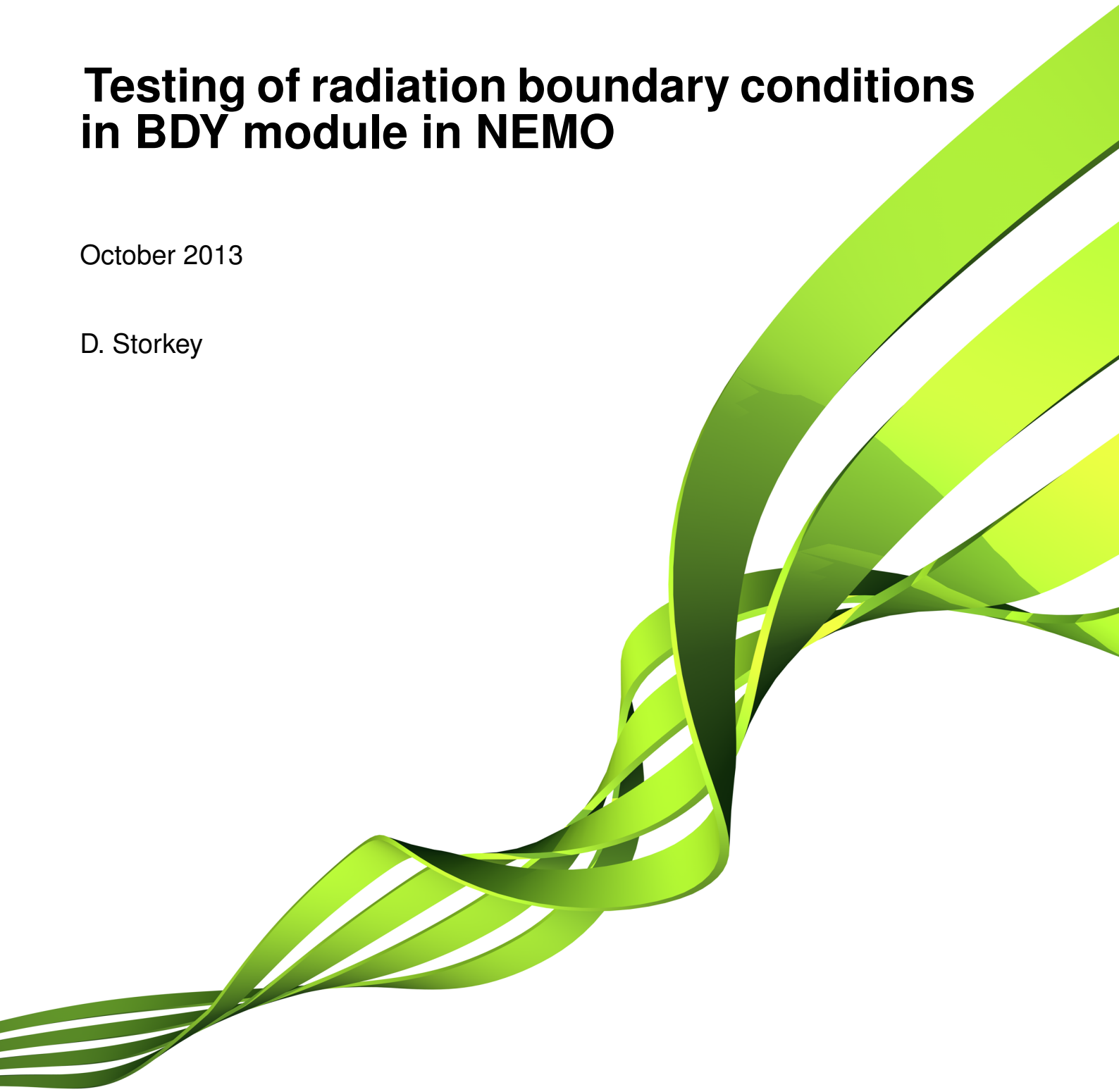

# Contents

# 1 Introduction

As part of the work to merge the OBC and BDY modules in NEMO, a version of the adaptive radiation-relaxation scheme coded in OBC has been coded and tested in BDY.

The version coded in BDY is based on the algorithm described by Marchesiello, McWilliams and Shchpetkin (2001), hereafter MMS. This differs in several ways from the version coded in OBC, notably:

- The MMS scheme uses forward timestepping with implicit timestepping for the normal component of radiation. The OBC scheme uses an explicit, leapfrog timestep.
- The MMS scheme applies the radiation condition to the barotropic and baroclinic velocities separately. In OBC the radiation condition is applied to the full velocity field.
- In OBC the radiation velocity used for the boundary condition for the tracer fields is calculated from the tangential velocity field. In BDY the tracer boundary condition uses a radiation velocity calculated from the tracer fields.

A full derivation of the scheme as coded in BDY is given in Appendix A. Testing was performed using an idealised equatorial soliton case and a realistic $\frac{1}{12}^{o}$ Mediterranean configuration. Testing was performed using NEMO version 3.5, revision 8479 of the central Paris repository.

# 2 Tests with idealised equatorial soliton

MMS describe tests of the open boundary condition with the idealised equatorial soliton described in Haidvogel and Beckmann (1999). This test case was set up in NEMO as described in MMS and Haidvogel and Beckmann. The soliton is a solution of the shallow water equations on an equatorial $\beta$-plane. Since NEMO does not have an option to solve the shallow water equations in isolation, the test case was set up as a 3D model with 150km horizontal resolution and 4 ocean levels in the vertical (total depth of 40 cm). Following Haidvogel and Beckmann, the sea surface height and velocities were initialised with the zeroth order soliton solution. The initial sea surface height field is shown in Figure (1). Temperature and salinity were initialised to be uniform. The model was integrated as an inviscid model, ie. with no explicit lateral or vertical viscosity and with no lateral or bottom friction. The model was integrated forward with a timestep of 30 minutes. After 40 non-dimensionalised time units (=68.4 days), dispersion has caused a loss of peak amplitude of around 13% which is comparable to the results that Haidvogel and Beckmann find with the SCRUM model at the same resolution.

Following MMS, open radiative boundary conditions are set up on all four boundaries with the soliton initialised about 10000km from the western boundary. The following cases were tested: the standard OBC (NPO) radiation, the BDY NPO radiation condition, and the BDY fully oblique radiation

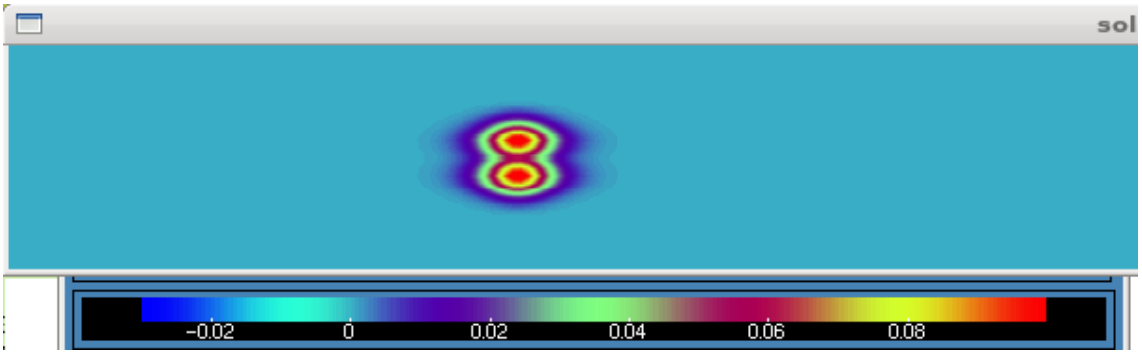


Figure 1: Figure showing the initial sea surface height field (m) for the soliton test case. The soliton is initialised at 10000km from the western boundary and has an initial amplitude of about 0.1m.

condition. In all cases a weak relaxation to initial conditions (ie. zero velocities) was applied with a 1000 day timescale. Tests were performed with both the filtered and timesplit options for the barotropic solution with the linear free surface approximation.

The OBC condition was found to be unstable for the timesplit barotropic solution, blowing up very quickly on the north and south boundaries. Results for the other experiments are shown in Figures (4) and (5). Figure (4) shows the sea surface height field after 200 days integration. For all schemes the interaction of the soliton with the western boundary produces a kelvin wave travelling east. In OBC (filtered free surface) the peak amplitude of this kelvin wave is about half of the initial amplitude of the soliton, but for all the BDY tests the amplitude of the kelvin wave is similar to the amplitude of the initial soliton. Figure (5) shows the evolution of the area-averaged kinetic energy, potential energy and total energy for the same four cases. For a perfect radiative scheme the soliton would be absorbed at the boundary and the total energy in the model domain fall to zero. For OBC with the filtered free surface the total energy falls to less than half of its initial value when the soliton interacts with the boundary at about day 150, and then rises as noise is generated at the boundary. For the BDY schemes no significant reduction in the total energy is apparent at day 150. Note that both OBC and BDY are eventually unstable for the filtered free surface case when the reflected kelvin wave interacts with the eastern boundary.

# 3 Tests with MED12 configuration

A second set of tests were performed with a $\frac{1}{12}^{o}$ model of the Mediterranean Sea (MED12). As shown in Figure (2), the model has north, west and south open boundaries in the Atlantic in order to allow the Gibraltar exchange to evolve naturally. The bathymetry was modified as recommended in Madec (2008), section 8.4, such that there was no normal gradient of the bathymetry over the outermost 4 grid cells and artificial islands were set up at the north-west and south-west corners of the domain to avoid having open boundaries at corners. The model was initialised with climatological temperature and salinity fields and spun up from rest, forced with fluxes from the Met Office NWP

model.

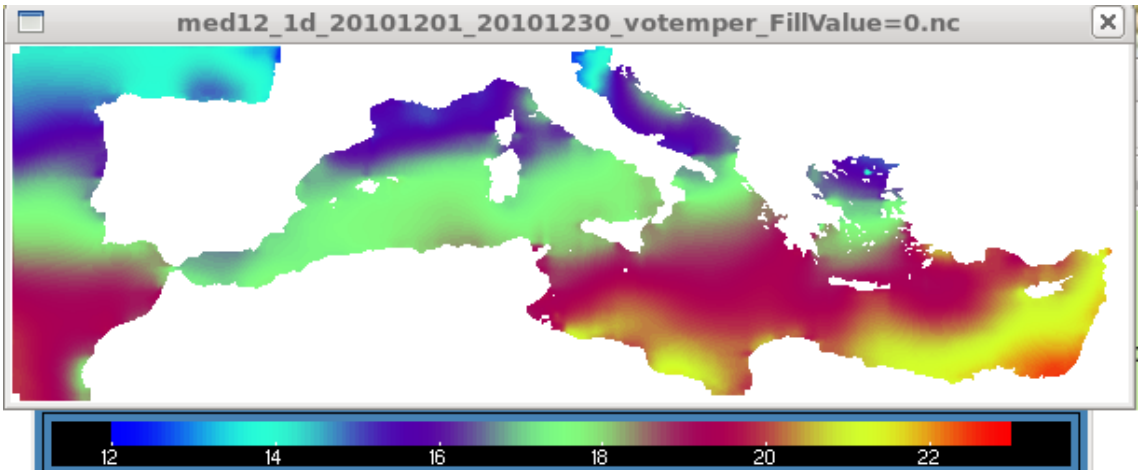


Figure 2: Figure showing the domain and the initial temperature field (deg C) for the MED12 configuration.

Tests were performed with adaptive radiation boundary conditions from OBC and BDY setting a relaxation timescale of 1000 days at outflow points and 1 day at inflow points. Initial conditions were used as external data for the relaxation. The fully oblique radiation condition in BDY was found to be unstable in this configuration; results shown here are for the NPO version. For the BDY tests it was found necessary to use the volume constraint option, that is a correction is added to the normal velocities at the boundaries to prevent the sea surface height from drifting. This was not necessary for the OBC tests, but the OBC results shown here have the volume constraint activated to make the experiments as close as possible to the BDY experiments.

Figure (6) show velocity components at 100m after 30 days spin up. The top two plots show results from using radiation conditions on all variables in OBC and BDY. In both cases spurious tangential velocities have spun up at the open boundaries. The tangential velocities on the western boundary are larger in BDY and there are signs that a barotropic eddy is spinning up. A further test was done where the radiative conditions were applied just to the velocity field and the flow relaxation scheme (FRS) applied to the tracer fields (bottom right of Figure (6)). In this case the large velocities along the western boundary do not spin up, but there are tangential velocities along the edge of the relaxation zone visible in the surface fields (not shown). A further test where FRS is applied to all variables gives quite similar results (bottom left of Figure (6)).

# 4 Conclusions

In the two test cases described, the radiation-relaxation algorithm coded in BDY does not seem to perform as well as the scheme coded in OBC. It may be that there is still a bug or mistake in the algorithm, or it may be that the MMS version of the algorithm does not fit so well in NEMO. For example the MMS scheme uses forward timestepping and NEMO uses a leapfrog timestep. It

would be interesting to revert the differences outlined in Section 1 to see if the OBC results were recovered. Tests have been done applying the radiation condition to the full velocity field instead of applying the radiation condition to the barotropic and baroclinic components separately. This did not change the results very much. To revert the other two changes would require a complete re-coding and there has not been time to try this.

## References

Haidvogel, D.B. and Beckmann, A. (1999), *"Numerical Ocean Circulation Modelling"*, Imperial College Press, ISBN 1-86094-114-1

Madec G. (2008) *"NEMO ocean engine"*. Note du Pole de modlisation, Institut Pierre-Simon Laplace (IPSL), France, No 27 ISSN No 1288-1619

Marchesiello, P., McWilliams, J.C. and Shchepetkin, A. (2001), *"Open boundary conditions for long-term integration of regional ocean models"*, Ocean Modelling **3** pp 1-20

## A Derivation of formulation of boundary condition from Marchesiello et al as implemented in NEMO.

The following gives the derivation of the boundary condition from Marchesiello et al (2001) (hereafter MMS) as implemented in the BDY module in NEMO.

The adaptive Orlanski condition solves a wave plus relaxation equation at the boundary:

$$\frac{\partial \phi}{\partial t} + c_x \frac{\partial \phi}{\partial x} + c_y \frac{\partial \phi}{\partial y} = -\frac{1}{\tau}(\phi - \phi^{ext}) \tag{1}$$

where $\phi$ is the model field, $x$ and $y$ refer to the normal and tangential directions to the boundary respectively, and the phase velocities are diagnosed from the model fields as:

$$c_x = -\frac{\partial \phi}{\partial t} \frac{\partial \phi / \partial x}{(\partial \phi / \partial x)^2 + (\partial \phi / \partial y)^2} \tag{2}$$

$$c_y = -\frac{\partial \phi}{\partial t} \frac{\partial \phi / \partial y}{(\partial \phi / \partial x)^2 + (\partial \phi / \partial y)^2} \tag{3}$$

(As noted by MMS, this is a circular diagnosis of the phase speeds which only makes sense on a discrete grid). Equation (1) is defined adaptively depending on the sign of the phase velocity normal

 

to the boundary $c_x$. For $c_x$ outward, we have

$$\tau = \tau_{out} \tag{4}$$

For $c_x$ inward, the radiation equation is not applied:

$$\tau = \tau_{in} \;\; ; \;\; c_x = c_y = 0 \tag{5}$$

Generally the relaxation time scale at inward propagation points is set much shorter than the time scale at outward propagation points so that the solution is constrained more strongly by the external data at inward propagation points. The "normal propagation of oblique radiation" or NPO approximation involves assuming that $c_y$ is zero in equation (1), but including this term in the denominator of equation (2). Both versions of the scheme are options in BDY. Equations (1) - (5) correspond to equations (13) - (15) and (2) - (3) in MMS.

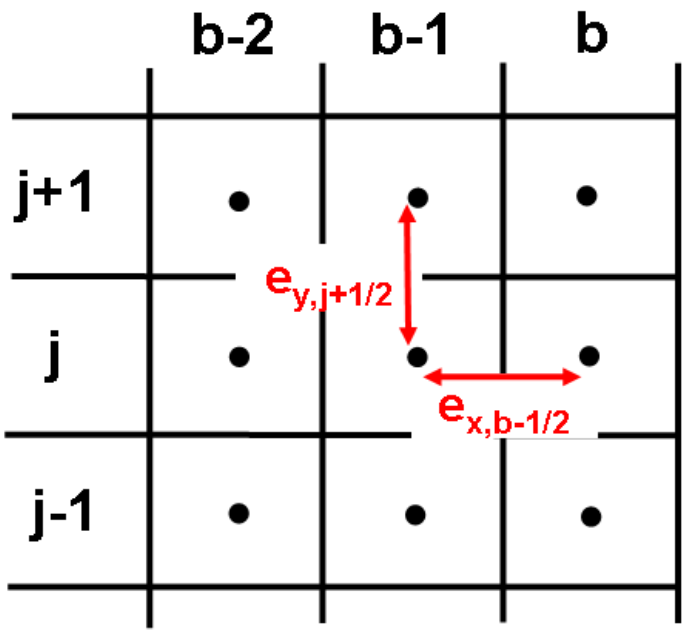


Figure 3: Figure showing the indexing convention near the boundary for the example of an eastern boundary. The normal index $b$ decreases inward from the boundary. The tangential index $j$ increases in the same sense as the relevant model index. Spatial scale factors $e_x$ and $e_y$ are defined at half-integer points relative to the model field $\phi$.

MMS use a forward timestepping scheme with implicit timestepping for the normal component of propagation. In the context of the NEMO leapfrogging scheme we do a forward timestep between the "before" and "after" timesteps in the same way as is done for the diffusion terms in NEMO.

Discrete version of (1), not expanding $c_x$ and $c_y$ for now:

$$\frac{\phi_{b,j}^{n+1} - \phi_{b,j}^{n-1}}{2.\Delta t} = -\frac{c_x}{e_{x,b-1/2}} \left[\phi_{b,j}^{n+1} - \phi_{b-1,j}^{n+1}\right] - \frac{c_y}{e_{y\_ups}} \left[\Delta\phi_{y\_ups}^{n-1}\right] - \frac{1}{\tau}\left[\phi_{b,j}^{n-1} - \phi^{ext}\right] \tag{6}$$

where $b$ and $j$ are the indices in the normal and tangential directions respectively as shown in Figure (3). The $b$ index decreases as you move inward from the boundary. The $j$ index increases in the same sense as the relevant model grid index. The superscripts refer to the time level, with $n-1$ referring to the "before" time level and $n+1$ referring to the "after" time level. $\Delta t$ is the timestep (corresponding to NEMO $rdt$) and $\Delta\phi_{y\_ups}$ and $e_{y\_ups}$ are defined as follows:

$$\Delta\phi_{y\_ups} = \phi^{n-1}_{b,j} - \phi^{n-1}_{b,j-1} \text{ and } e_{y\_ups} = e_{y,j-1/2} \text{ if } r_y > 0, \tag{7}$$

$$\Delta\phi_{y\_ups} = \phi^{n-1}_{b,j+1} - \phi^{n-1}_{b,j} \text{ and } e_{y\_ups} = e_{y,j+1/2} \text{ if } r_y < 0, \tag{8}$$

where

$$r_x = \frac{2.c_x.\Delta t}{e_{x,b-1/2}}; \quad r_y = \frac{2.c_y.\Delta t}{e_{y\_ups}} \tag{9}$$

Solving equation (6) for $\phi^{n+1}_{b,j}$ we get:

$$\left(1 + \frac{2.c_x.\Delta t}{e_{x,b-1/2}}\right)\phi^{n+1}_{b,j} = \phi^{n-1}_{b,j} + \frac{2.c_x.\Delta t}{e_{x,b-1/2}}\phi^{n+1}_{b-1,j} - \frac{2.c_y.\Delta t}{e_{y\_ups}}\Delta\phi^{n-1}_{y\_ups} - \frac{2.\Delta t}{\tau}\left[\phi^{n-1}_{b,j} - \phi^{ext}\right]$$

$$\Rightarrow \phi^{n+1}_{b,j} = \frac{1}{1+r_x}\left[\left(1 - \frac{2\Delta t}{\tau}\right).\phi^{n-1}_{b,j} + r_x.\phi^{n+1}_{b-1,j} - r_y.\Delta\phi^{n-1}_{y\_ups} + \frac{2\Delta t}{\tau}.\phi^{ext}\right] \tag{10}$$

Writing the discrete version of (2),

$$c_x = -\frac{\Delta\phi_t}{2.\Delta t}.\frac{\Delta\phi_x/e_{x,b-1.5}}{(\Delta\phi_x/e_{x,b-1.5})^2 + (\Delta\phi_y/e_{y,j\pm1/2})^2} \tag{11}$$

where

$$\Delta\phi_t = \phi^{n+1}_{b-1,j} - \phi^{n-1}_{b-1,j} \tag{12}$$

$$\Delta\phi_x = \phi^{n+1}_{b-1,j} - \phi^{n+1}_{b-2,j} \tag{13}$$

$$\Delta\phi_y = \phi^{n-1}_{b-1,j} - \phi^{n-1}_{b-1,j-1} \text{ if } (\Delta\phi_t.\Delta\phi_{y\_centred}) > 0 \tag{14}$$

$$\Delta\phi_y = \phi^{n-1}_{b-1,j+1} - \phi^{n-1}_{b-1,j} \text{ if } (\Delta\phi_t.\Delta\phi_{y\_centred}) < 0 \tag{15}$$

and

$$\Delta\phi_{y\_centred} = \frac{1}{2}\left(\frac{\phi^{n-1}_{b,j} - \phi^{n-1}_{b,j-1}}{e_{y,j-1/2}} + \frac{\phi^{n-1}_{b,j+1} - \phi^{n-1}_{b,j}}{e_{y,j+1/2}}\right) \tag{16}$$

Equations (10) - (16) are the same as MMS equations (4) - (11) with a couple of exceptions:

- I have included the scale factors from the curvilinear grid in the expressions for the spatial derivatives. If the grid is uniform and isotropic, ie. $e_x = e_y = \text{constant}$ then the scale factors cancel in the expressions for $r_x$ and $r_y$ and the MMS equations are recovered.
- Equations (14) - (16) differ from MMS equations (10) and (11). Instead of the centred difference in the upstream criterion I use an average of two offset derivatives. This should almost

always give the same result and allows masking of the spatial derivatives which is particularly important for the tracer fields.

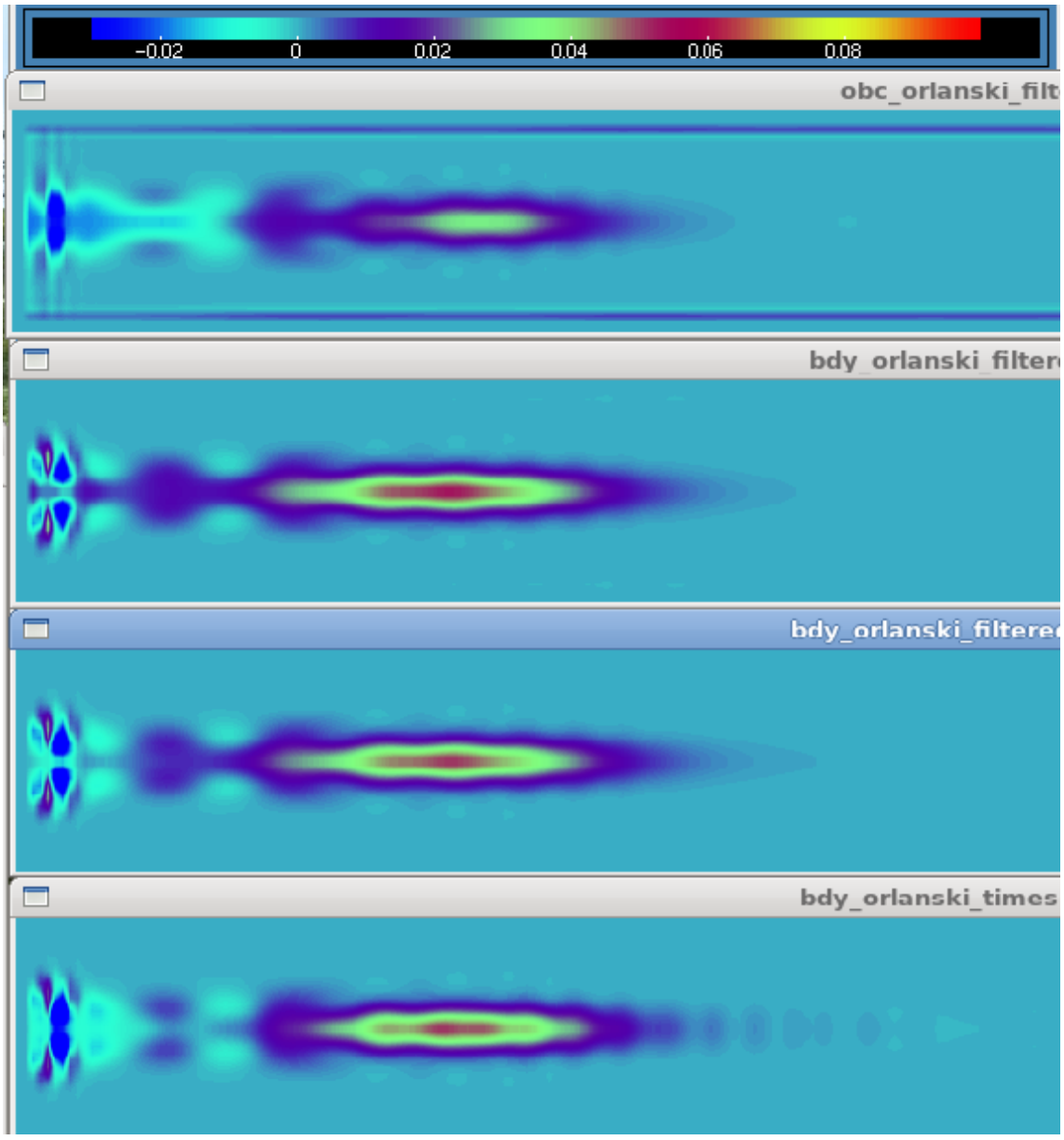


Figure 4: Figure showing the sea surface height field (m) after 200 days integration, subsequent to the interaction of the soliton with the western boundary. From top to bottom: OBC with filtered free surface; BDY NPO with filtered free surface; BDY fully oblique with filtered free surface; BDY NPO with timesplit free surface. In all cases a kelvin wave results from the interaction of the soliton with the boundary. For OBC the amplitude of the kelvin wave is about half the amplitude of the soliton; for BDY the amplitude of the kelvin wave is about the same as the amplitude of the soliton.

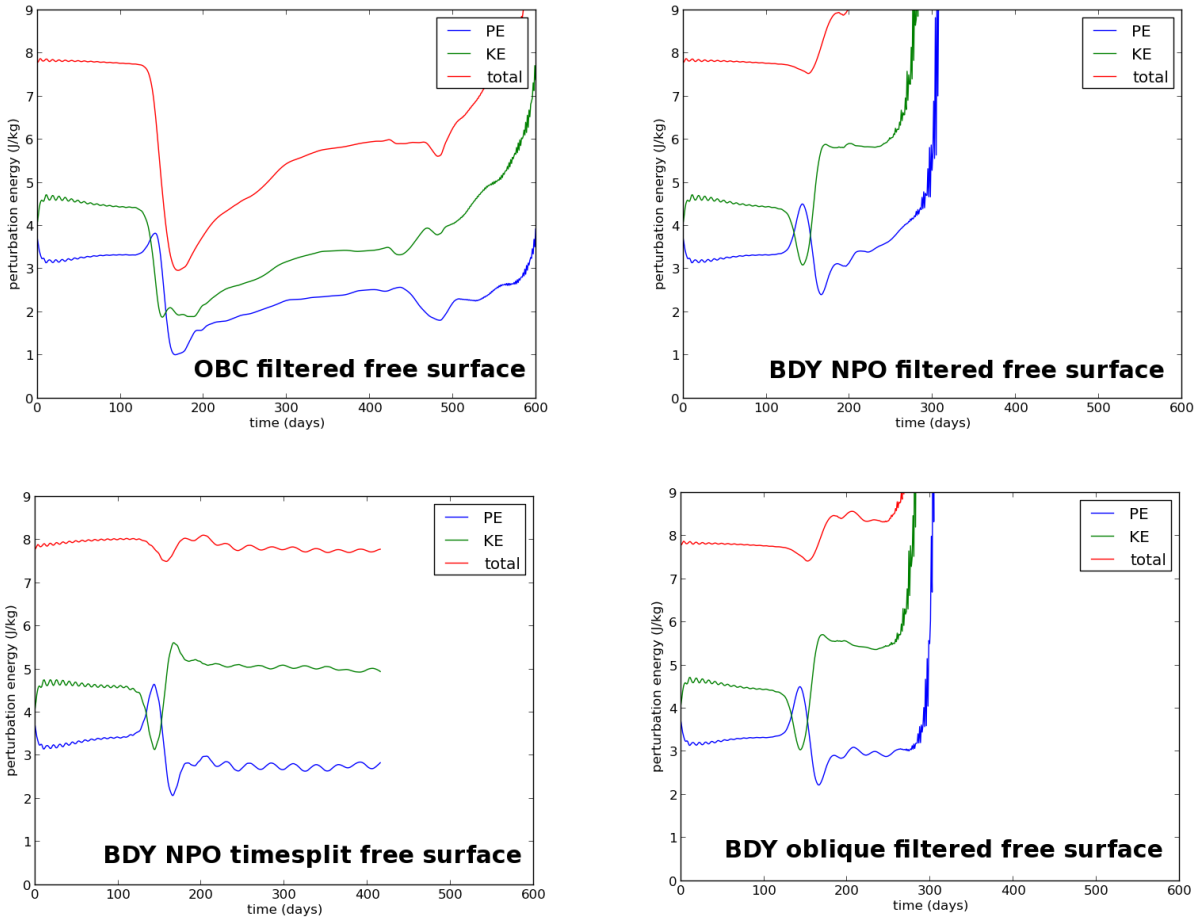


Figure 5: Timeseries of the area-integrated potential energy, kinetic energy and total energy for the four experiments shown in Figure (4). For a perfect radiation scheme the total energy should fall to zero when the soliton hits the open boundary (about day 150). For OBC there is an initial reduction of the total energy of over 50% but there is little reduction in the total energy for any of the BDY cases. The perturbation potential energy and kinetic energy were calculated as in Gill (1982), equation (5.7.4) ignoring a factor of $\frac{1}{2}\rho$ in each case.

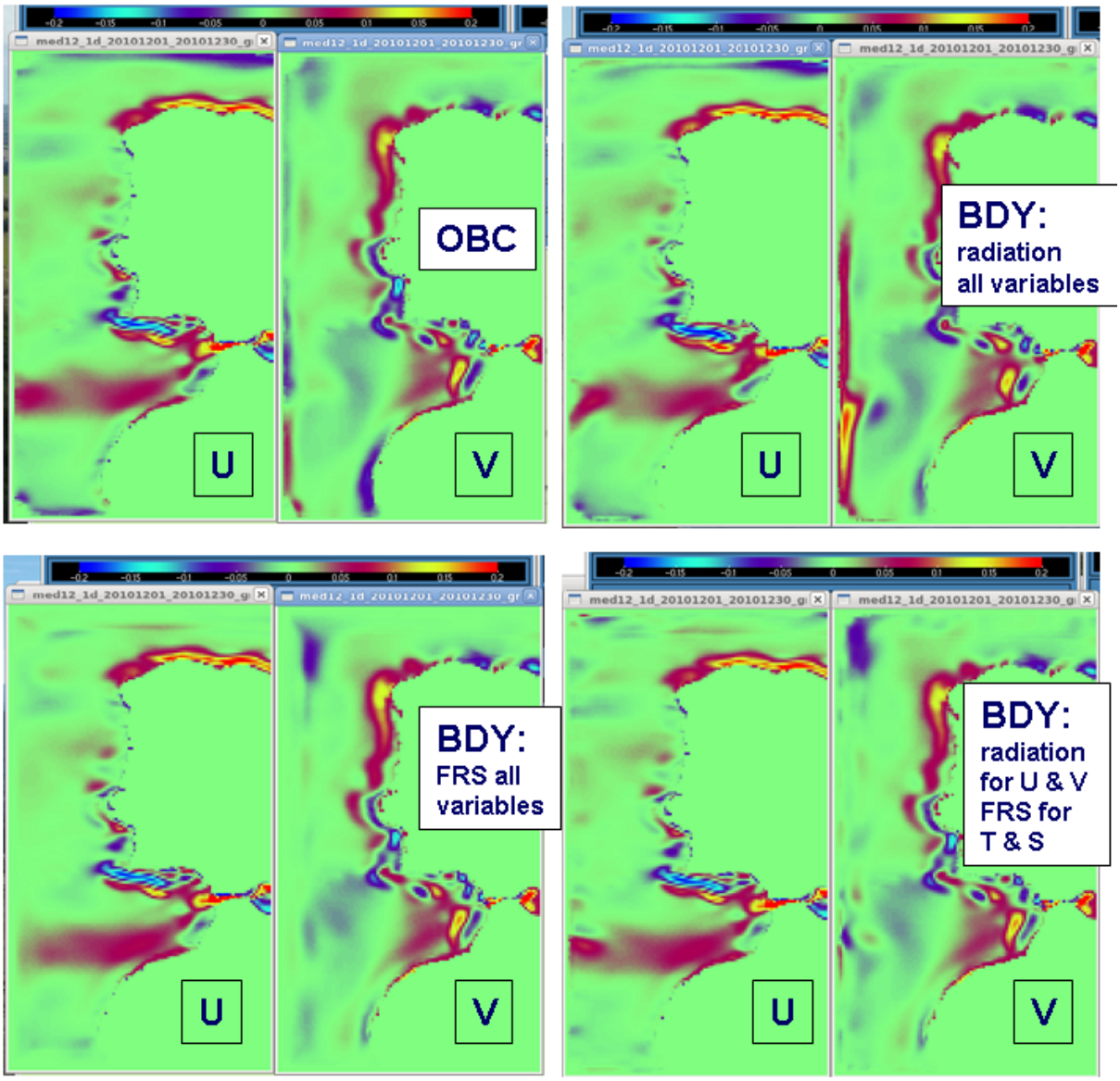


Figure 6: Figure showing U and V components of velocities at 100m for the MED12 test after 30 days spin up. Tangential velocities are visible along the north and south boundaries for both OBC and BDY. They are reduced significantly in BDY if FRS boundary conditions are applied to the tracer fields.

**Met Office**
FitzRoy Road, Exeter
Devon, EX1 3PB
UK

Tel: 0870 900 0100
Fax: 0870 900 5050
enquiries@metoffice.gov.uk
www.metoffice.gov.uk

Produced with the Met Office LaTeX template v2.0.0